

Sketch Video Synthesis

Yudian Zheng
University of Saarland

Xiaodong Cun[†]
Tencent AI Lab

Menghan Xia
Tencent AI Lab

Chi-Man Pun
University of Macau

<https://sketchvideo.github.io>

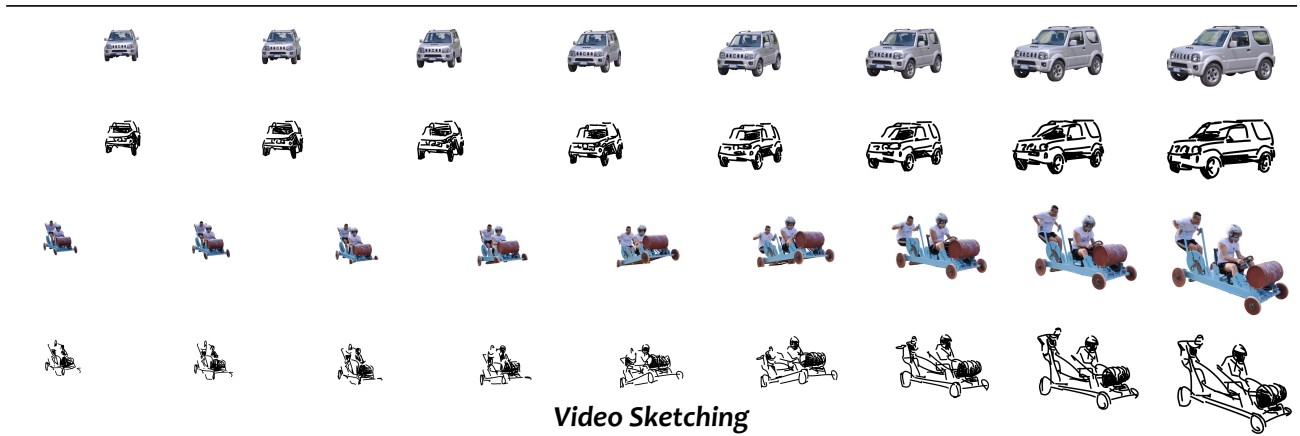


Figure 1. Given an input video (of the foreground object), we introduce a novel method for sketching the video using Bézier Curves so that the video can be represented by scalable vector graphics (SVG). The generated sketch video maintains semantic alignment with the input and exhibits temporal consistency. The flexibility of SVG allows for various rendering techniques, including resizing, color filling, and overlaying doodles on the original background images, enabling the creation of diverse artistic effects.

Abstract

Understanding semantic intricacies and high-level concepts is essential in image sketch generation, and this chal-

lenge becomes even more formidable when applied to the domain of videos. To address this, we propose a novel optimization-based framework for sketching videos represented by the frame-wise Bézier Curves. In detail, we first propose a cross-frame stroke initialization approach to warm

[†] Corresponding author.

up the location and the width of each curve. Then, we optimize the locations of these curves by utilizing a semantic loss based on CLIP features [34] and a newly designed consistency loss using the self-decomposed 2D atlas network [22]. Built upon these design elements, the resulting sketch video showcases impressive visual abstraction and temporal coherence. Furthermore, by transforming a video into SVG lines through the sketching process, our method unlocks applications in sketch-based video editing and video doodling, enabled through video composition, as exemplified in the teaser.

1. Introduction

Freehand drawing is a widely adopted method for quickly prototyping ideas across various domains [15, 47]. This approach embodies simplicity, abstraction, and adaptability, empowering individuals to effectively express their concepts. Furthermore, skilled artists can develop distinctive artistic styles through freehand drawing. While sketching is a common practice for images, often using formats like scalable vector graphics (SVG), there has been limited exploration of its application in the context of sketching videos. This uncharted territory makes the exploration of sketch videos an intriguing and meaningful endeavor.

While traditional approaches, such as edge detection methods [6, 46] excel in rendering realistic sketches, they struggle to create more expressive and abstract representations due to their reliance on mathematical and geometric operations. In an attempt to incorporate semantic awareness, previous sketching methods have attempted to learn human-like sketches from a collected dataset in different levels of abstraction and styles [4, 21, 28] at the pixel level. While these data-driven methods imitate human sketches, the requirements and quality of the relevant datasets restrict the output. As introduced by recent image sketching works [40, 41], line drawings are defined using the control points of Bézier Curves and are optimized to represent the scene. These methods employ multi-scale deep perceptual losses [34] to bridge the gap between generated sketches and real scenes, bypassing the constraints of traditional datasets and yielding diverse results. We follow these frameworks to represent video sketches in SVG format. However, if we simply apply image-based sketching [41] in a frame-wise manner without careful consideration, the strokes will converge into local minima rapidly. Additionally, the flickering issue of generated video is not easily resolved through conventional video deflickering algorithms [25, 26], especially when dealing with vector graphics.

To overcome the challenges mentioned above, we introduce an innovative optimization-based framework aimed at generating sketch videos in SVG format that exhibit both semantic alignment and temporal consistency. To achieve

this goal, we leverage Neural Layered Atlas (NLA) [22] to our tasks for multiple purposes. NLA is first proposed for video editing, it maps each point in video to a uniform global UV map, so that it can guarantee the correspondences across frames and help for temporal point consistency. In detail, the process of generating a high-quality video sketch involves careful initialization and continuous optimization of the sketch video. We begin by carefully selecting the initial locations for candidate points, where an effective initialization is crucial for avoiding unfavorable local minima [41] and accurately conveying the video’s semantics. To achieve this, our initialization approach utilizes semantic-aware edges, derived from salient maps obtained from the combination of CLIP features [34] and XDoG edge detection [43]. Subsequently, these selected points are propagated to all frames and optimized to their initial positions using a pre-trained NLA. Then, we optimize the location of these points using several losses so that they can ensure both semantic alignment and temporal consistency. We transform the candidate points to Bézier Curves and utilize a differentiable rasterizer [29] to render them to the frame-wise images. For semantic abstraction, we utilize the pre-trained CLIP image encoder as a feature extractor and compute losses between the rendered one and the real video frame. For temporal consistency, we ensure consistency of vector points via the pre-trained NLA [22] so that they can be consistent from a global view. Based on these techniques, the proposed method can successfully generate the abstraction sketches of the specific given video.

In addition to streamlining the process of sketching videos, our approach paves the way for various video applications. For instance, it allows for the creation of colorful videos by applying drawing techniques to a single frame. Furthermore, our method introduces novel possibilities in video editing, such as substituting the original content by integrating sketches into the scenes. Additionally, our approach enables the generation of video doodles to enhance other video content.

The contribution of this paper can be summarized as:

- We first tackle the problem of generating scalable abstract videos via several Bézier curves.
- By utilizing the consistency of pre-trained video implicit representation [22], we propose a novel point initialization method and a temporal consistency loss for video sketching synthesis.
- Our method generates the animated SVG from the input video, enabling multiple new applications of video editing and doodles.

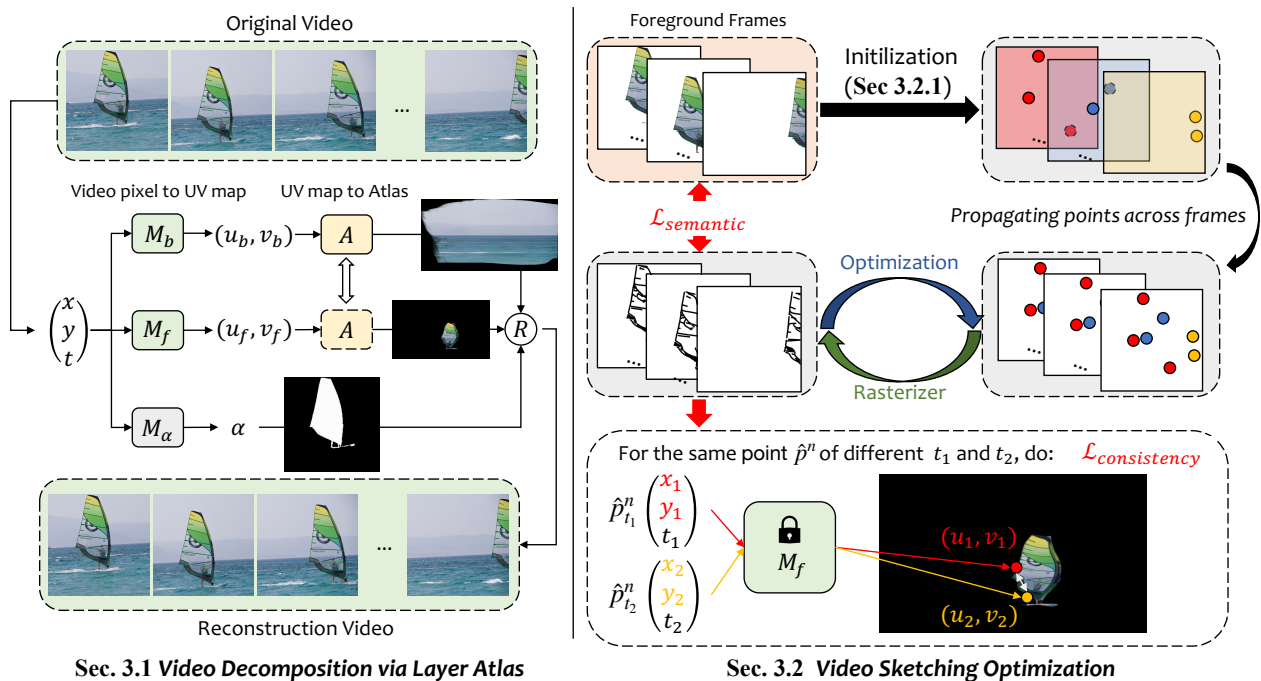


Figure 2. **The pipeline of the whole framework.** Firstly, we train a layer atlas to decompose the video into the trained layer atlas. Then, we optimize the location of the generated frames via the proposed novel initialization methods and consistency loss.

2. Related Work

2.1. Doodling and Abstraction

Doodling and abstraction are common forms of artistic expression that use few and sparse curves to depict objects or scenes abstractly. Early works in sketching, such as traditional edge detection methods [6, 46], effectively describe the structure and semantics of images. While these methods produce clear and coherent sketch videos, they lean towards excessive realism, often neglecting the artistic preferences of viewers. Combining edge detection methods with line drawing video stylization [3] generates abstract images, but it often overlooks the holistic aspect of video frames and loses video consistency. Recent data-driven methods primarily focus on generating human-like sketches through domain adaptation using carefully curated datasets [1, 16]. These methods offer the ability to create various styles and levels of abstraction. However, the resulting style is often closely tied to the specific dataset characteristics, making it less suitable for unstructured and previously unseen data. Extending these methods to handle videos, which are typically supervised by image datasets, is also a challenging endeavor. Another method, such as video doodling [49], is used in sketch addition on video, but it is not satisfied with a global level of abstraction.

2.2. Vector Sketching Generation

There are some image-to-vectors methods [7, 8, 35] that can typically produce pixel-aligned results. However, sketching demands a higher level of abstraction and greater continuity between lines. Recent advancements in differential gradient algorithms, such as DiffVG [29], have made it feasible to optimize images and even SVG representations within the pretrained CLIP [34] space. For example, CLIPDraw [13] explores the potential of optimizing SVG images to generate drawings that closely align with text prompts, leveraging the guidance of CLIP. Similarly, Tian and Ha [39] have designed an evolutionary algorithm to abstract images using vector triangles.

Regarding closely related works, CLIPasso [41] specifically applies the technique of CLIPDraw [13] to generate object sketches, and CLIPascene [40] extends the optimization process to incorporate background elements. Furthermore, similar optimization methods have been employed in the domain of artistic fonts [18] with the diffusion model [36]. Text-based vector generation has attracted research attention, as evidenced by Wu *et al.* [45], who propose a transformer-based method for generating icons from text auto-aggressively. Different from the vectorization method for images, our approach focuses on generating sketch videos that need to keep temporal consistency, and directly using the image-based method will fall into local minimal due to

initialization.

2.3. Video Editing and Temporal Consistency

Video editing and stylization have a long history within the computer vision and graphics communities. Various attempts have been made to achieve stylization [11, 19]. However, these methods may face challenges in maintaining tracking consistency. Since frame-wise techniques can generate high-quality stylized images [14, 20], it has become a common practice to employ neural networks for reducing temporal inconsistencies as a post-processing step [5, 24, 26, 27]. Nonetheless, it is important to note that style transfer techniques primarily rely on measuring perceptual distance [50], which can result in imperfect stylization due to a lack of deep comprehension at the semantic level. Some recent works have shown improved consistency, but often within specific domains, such as portrait videos [12, 48]. For local video editing, layer-atlas-based methods [2, 22] present a promising approach by allowing video editing on a flattened texture map and generating results through color-wise mapping.

More recent approaches have explored video editing using diffusion models [36]. These models offer stronger priors for editing using text. *e.g.*, Gen1 [10] trains a conditional model for depth and text-guided video generation, allowing on-the-fly appearance editing of generated images. Several methods [23, 31, 33, 44] leverage pre-trained text-to-image diffusion models for zero-shot or one-shot video editing. Although current methods have shown promising results for image pixels, there is still a lack of techniques for generating vector video sketches.

3. Methods

Our approach primarily aims to generate the sketch representation of the objects in video, which can be represented through multiple vector strokes. Each stroke is represented as the four points Bézier Curves, where we focus on maintaining both semantic accuracy and temporal consistency. To achieve, this goal, as shown in Figure 2, we first decompose a video into a 2D representation using layer atlas [22] (Sec. 3.1). Then, we introduce a new framework to optimize the location of these points in Sec. 3.2. Finally, we give some potential applications in Sec. 3.3.

3.1. Preliminary: Video Decomposition via Layer Atlas

Unlike previous video synthesis and editing tasks [10, 42], our method focuses on optimizing the positions of discrete points within curves to ensure consistent behavior across frames. Therefore, using image-based frame deflickering methods [25, 26] directly becomes challenging. To address

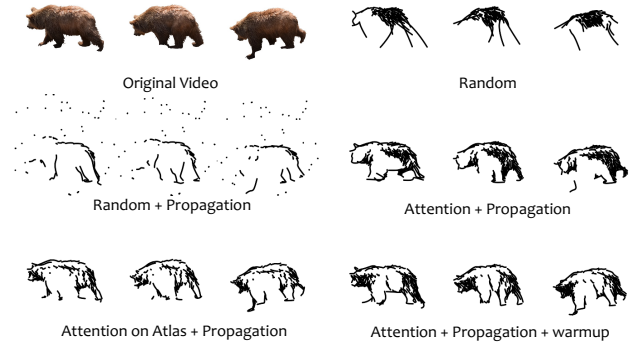


Figure 3. The influence of different initialization methods.

this, we leverage the trained representation of previous consistent video editing method, *i.e.*, Neural Layered Atlas (NLA [22]), to maintain point consistency.

As shown in the left part of Fig. 2, the Neural Layered Atlas (NLA) treats the video as a spatial-temporal 3D volume, where each 3D coordinate within the video is mapped onto the foreground (or background) 2D UV -maps through a Multi-Layer Perceptron (MLP). Additionally, an extra MLP is employed to assign color values to a given 2D UV location. To formalize this, let’s consider a video pixel as $p = (x, y, t)$, where x and y are the coordinates of the pixel within the t -th frame. NLA generates the 2D UV maps for foreground and background individually as shown in Fig 2. It uses M_f and M_b to map 3D coordinate p to a 2D location in foreground UV -map as (u_f, v_f) , and in background UV -map as (u_b, v_b) separately. The MLP M_α indicates the ownership of the points (foreground or background) according to the motion prior and the pre-defined mask losses. Subsequently, a shared MLP A is trained to map the (u, v) to the corresponding color in RGB space, ensuring that the same pixel in the real world should have the same color.

This comprehensive process facilitates the video reconstruction. After training, the mapping MLPs M_f and M_b indicate the correspondence between points in the video and specific points within the holistic UV -map, aligning with our requirements for curve mapping consistency. Our method adheres to the original video decomposition approach of the layer atlas. For more specific information regarding training and loss functions, detailed insights can be found in [22].

3.2. Differentiable Optimization for Video Sketch

In this section, we give the details on how to generate a sketch video in our framework. Formally, given a real video $\{\mathcal{I}_1, \dots, \mathcal{I}_T\}$ contains T frames, we define the sketching video $\{\mathcal{S}_1, \dots, \mathcal{S}_T\}$ as a set of N strokes $\mathcal{S}_t = \{s_1, \dots, s_N\}$ for each frame. Each stroke s_i is defined as the two dimensional Bézier curves, where each curve is built via 4 control points $s_i = \{(x_i, y_i)^k\}_{k=1}^4$. We empirically use the same index i of stroke s_i in different sketches \mathcal{S}_t to represent

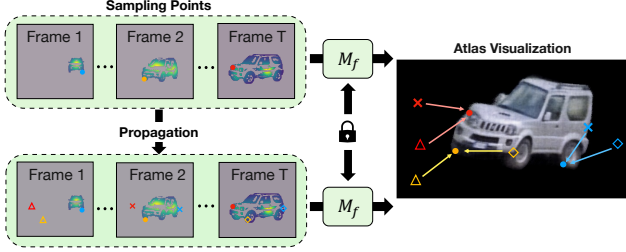


Figure 4. **Coordinate Initialization.** The initialized points are warmed up by optimizing the propagated points in different frames $\{\triangle, \triangle, \times, \times, \diamond, \diamond\}$ closer to the sampling points $\{\bullet, \bullet, \bullet\}$ on the atlas (by mapping MLP M_f).

the same curve across frames and only optimize their positions. All other curve-related attributes are following the previous image sketching method [41]. We then use a differentiable rasterizer \mathcal{R} from DiffVG [29] to transform the control points and attributes of Bézier Curves into a Scalable Vector Graphics (SVG) to represent the final sketch video. So the loss functions \mathcal{L} can be optimized between the real video and the sketches representation. The overall process can be represented as:

$$\arg \min_{(X,Y)} \sum_{t=1}^T \mathcal{L}(\mathcal{R}(S_t), \mathcal{I}_t), \quad (1)$$

where (X, Y) are all the coordinates of the control points $\bigcup_{i=1}^N \bigcup_{k=1}^4 (x_i, y_i)^k$ in the whole sketch video.

Subsequently, we first introduce our method on how to obtain the initial stroke settings on video (Sec. 3.2.1). Then, we elaborate on the particulars of rendering points into curves and optimize the entire video (sec. 3.2.2).

3.2.1 Strokes Initialization

The objective function of our abstraction is highly non-convex [41] since the optimization loss is based on rendered views in pixel differences [29]. Thus, attempting to optimize the location directly from random initialization often leads to the process getting trapped in local extrema, both in the image and video abstraction (as in Fig. 3). To overcome this challenge, CLIPasso [41] employs a saliency-guided initialization process, where strokes are sampled from the probability map. This map is generated by multiplying the saliency map via CLIP [34] feature with the image’s edge map extracted using XDoG [43], and then subjecting the result to softmax normalization. We argue this kind of initialization is hard to work in processing video since each frame has a variant attention map, where these varying initial points increase the difficulties of the point optimizations. Below, we give our solution step by step.

Point Propagation. We first aim to generate sparse key points across frames, which are used to represent the entire video. As shown in Figure 4, to build T frames SVG video

where each frame contains N strokes, we first apply saliency-guided initialization process [41] to sample N candidate points in each frame individually. Then, in order to obtain the initial points on video, we resample N points from the set of all $N \times T$ candidate points to build a cross-frame point set $P = \{p_1, \dots, p_N\}$. Here, p_n are 3D coordinates (x_n, y_n, t_n) , where n indicates the index of control points. Then, these cross-frame points are directly propagated to all frames so that each frame has the same spatial 2D initialization as $\hat{p}_n^t = (x_n, y_n, t)$.

Position Warmup. Since there can be offsets between the sampled points in different frames (e.g., the same color markings in various frames in Figure. 4), we employ an optimization-based approach to alleviate the differences between the propagated locations and the previously sampled positions on the UV maps by adjusting the propagated points only. This alignment is achieved through the use of the pre-trained atlas mapping network M_f to optimize the control points across frames on the atlas:

$$\mathcal{L}_{warmup} = \sum_{t=1}^T \sum_{n=1}^N \|M_f(\hat{p}_n^t) - M_f(p_n)\|_1, \quad (2)$$

In this situation, t represents the frame index, n signifies the control point index, p denotes the sampled points, and \hat{p} signifies the propagated points.

In practice, we warm up 300 iterations. This strategy helps us to find the most suitable initialization points. As shown in Fig. 3, random initialization (or solely attention-based methods [41] with similar results) yields poor performance due to the lack of correspondence between the same index points across the video. While propagating the points across different frames helps establish correspondence, it can still lead to a loss of focus on the object. Different attention strategies yield varying results, with frame-wise attention outperforming the attention map based on the atlas. This is because the atlas tend to exhibit distortions compared to the more realistic frames. Ultimately, the performance is further enhanced and becomes more accurate with the inclusion of a warm-up phase in the entire initialization process.

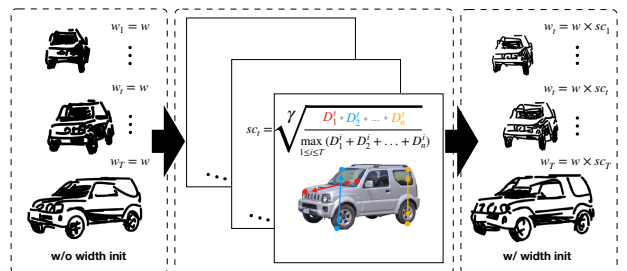


Figure 5. The width w_t of strokes in t -th frame is scaled by the variable sc_t , with initialized width w . The variable γ controls the contrast ratio of scale (default value is 3).

Curve Width Initialization. Additionally, we also initiate

the curve widths, considering that generated videos can involve significant motions and varying scales. Since more accurate stroke thickness enhances the representation of contours, instead of solely relying on the mask’s scale, we leverage the object’s distortion to estimate the appropriate scale. In detail, as depicted in Figure. 5, we randomly pair points in each frame to calculate the differences between points (here, we use all warmed-up points to create pairs). By computing the γ root of the weighted pair-wise differences on frame t (with γ defaulted to 3 as a measure of distortion in the 3D world), we derive a scale factor sc_t and curve width w_t :

$$sc_t = \gamma \sqrt{\frac{\sum_{n=1}^N D_n^t}{\max_{1 \leq i \leq T} (\sum_{n=1}^N D_n^i)}}, \quad (3)$$

$$w_t = sc_t \times w, \quad (4)$$

where w is the default width. Consequently, more distant objects are depicted with finer lines to capture intricate details and scale, while closer objects are outlined with thicker lines. This strategy enhances the quality of abstraction, particularly in scenarios involving substantial object motion.

3.2.2 Curves Optimization

Following a well-executed stroke initialization for the video, our aim is to optimize the curves based on the positions of their points. This optimization needs to ensure that the resulting sketch video maintains not only semantic similarities with the input video but also consistency across frames.

Firstly, we follow image-based sketching methods [41] to use the semantic-aware loss $\mathcal{L}_{semantic}$ to measure the differences between the generated points and the original video. $\mathcal{L}_{semantic}$ is based on the differences in multi-scale perception features extracted from the pre-trained CLIP image encoder [34]. Since CLIP is trained on a larger-scale dataset to align the text and image information through contrastive learning, the semantic information can be well-aligned. Formally, for the control points $\mathcal{S} = \{s_1, \dots, s_N\}$ where $s_i = \{(x_i, y_i)^k\}_{k=1}^4$ on each SVG, we optimize the positions of the control points based on the difference between the generated SVG and the actual input image \mathcal{I} via the l -th layer of pretrained CLIP Φ :

$$\mathcal{L}_{semantic} = \sum_{l \in \{3,5,9\}} \sum_{t=1}^T \|\Phi_l(\mathcal{R}(S_t)) - \Phi_l(\mathcal{I}_t)\|_1, \quad (5)$$

Here, T represents the total number of frames, and \mathcal{R} is the differentiable rasterizer as introduced above,

We also investigate the impact of variants of the CLIP encoders, specifically, the ViT [9] based and ResNet101-based models [17]. The ResNet101-based CLIP model exhibits



Figure 6. The differences in the choice of different semantic losses.

better performance with more local structures, while the ViT-based methods focus more on global features. Consequently, we default to using the ResNet101-based CLIP model, as depicted in Figure 6.

Besides, for our video sketching, we design a novel consistency loss to measure the consistency between the generated SVG videos. The most naive approach is to maintain control over the corresponding offsets to guarantee temporal consistency via optical flow [38, 42]. While optical flows are typically dense, they might suffer from potential errors, e.g., forward-backward consistency, and cumulative errors. Therefore, we employ the trained atlas network to obtain a panoramic view of the video. This allows each point in every frame of the video to be associated with a consistent global position on the atlas. By ensuring that related points and lines have consistent global positions, we can maintain the continuity of the video. Specifically, we use the pre-trained mapping network M_f from the layer atlas as shown in Figure 2, where for each control point $\hat{p}_n^{t_1}$ and its neighboring $\hat{p}_n^{t_2}$ of the same index n cross frames, where the $\mathcal{L}_{consistency}$ can be written as:

$$\mathcal{L}_{consistency} = \sum_{\hat{p}' \in \mathcal{N}(\hat{p})} \sum_{\hat{p} \in P} \|M_f(\hat{p}) - M_f(\hat{p}')\|_1, \quad (6)$$

After optimization, the same index n point \hat{p}_n cross frames will have a similar location in the 2D UV -map and it keeps consistency over frames.

Overall, the loss function can be written as:

$$\mathcal{L} = \omega_1 \mathcal{L}_{semantic} + \omega_2 \mathcal{L}_{consistency}, \quad (7)$$

where ω_1 and ω_2 are used to control the extent of semantics and consistency between sketches, respectively. We experimentally set $\omega_1 = 200.0$ and $\omega_2 = 3.0$.

3.3. Applications

SVG Editing. Because the generated video is in the form of SVG, our method has the ability to change the colors of all lines or fill specific lines within the video to create richer details in the visual content. As shown in Fig. 1, we can resize the canvas, paint all objects in orange, and fill the enclosed lines.

Video Editing and Doodling. Our method can also be employed for video editing and doodle creation. As shown in Fig. 1, after generating the SVGs, we can use inpainting techniques [37] to restore the original video and integrate the newly generated content into it. Additional video results are presented in the supp. video.

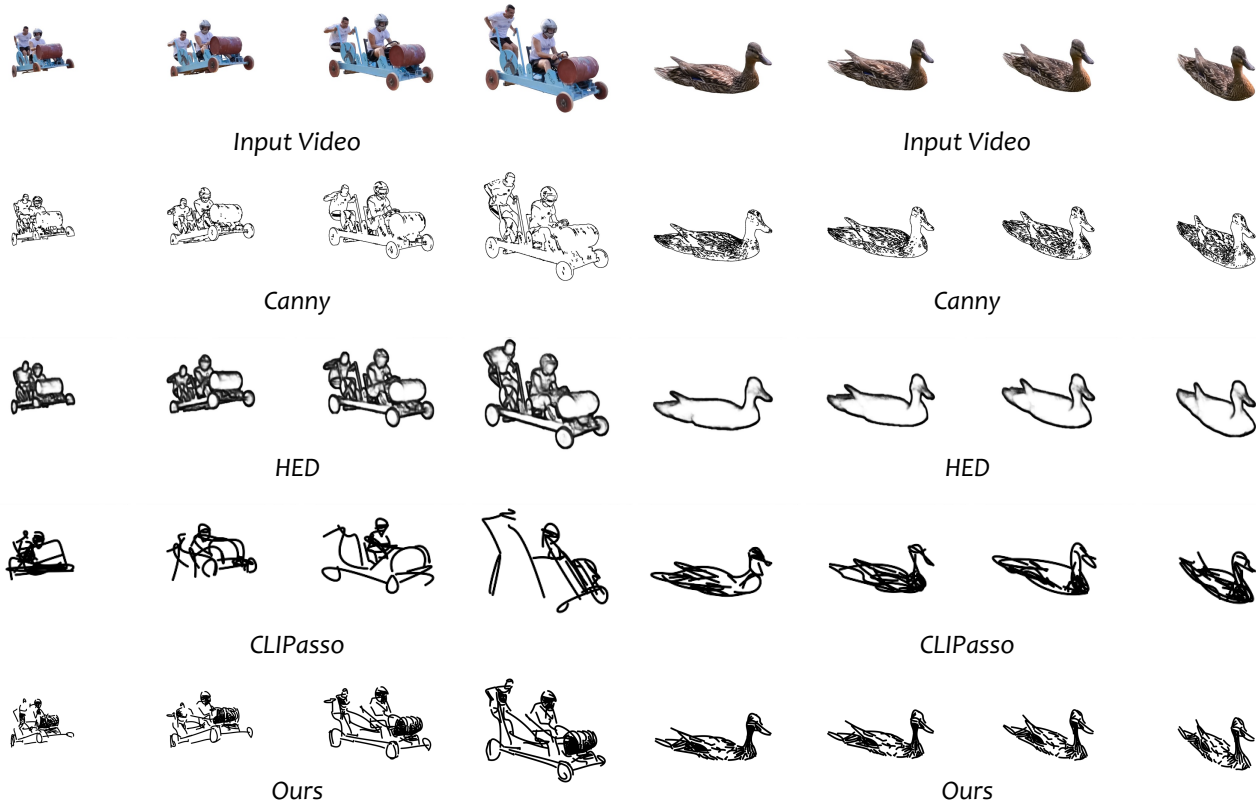


Figure 7. Comparisons with our methods and the states-of-the-art methods frame-wise methods, *i.e.*, frame-wise CLIPasso [41] and edge detection methods (canny [6] and HED [46]) on different frames of the videos.

4. Experiments

Our method is evaluated on DAVIS dataset [32], which provides foreground annotations for each frame. We also evaluate the proposed method on some self-collected datasets, utilizing the video matting method [30] to generate the foreground videos. In each case, we only used the first 50 frames in the video to generate the results for a fair comparison. Subsequently, we decompose the video into an atlas. For the optimization of sketching videos, we utilize the Adam optimizer with a learning rate of 1.0, following the approach of CLIPasso [41]. On average, optimizing a video sketch takes approximately 29 minutes, consuming around 19.5GB on a single NVIDIA GeForce RTX 3090 GPU.

4.1. Compare with state-of-the-art methods

As no previous video sketching methods exist, we employ some image sketching and edge detection techniques for comparison. For image abstraction, in particular, we compare with frame-by-frame CLIPasso [41]. Regarding edge detection, we assess against traditional edge detection techniques, namely Canny [6], as well as the deep learning-based method, HED [46]. As demonstrated in Figure 7, in comparison to CLIPasso, our approach exhibits improved temporal consistency while effectively preserving semantic informa-

tion. Concerning the edge detection methods, our proposed technique showcases superior semantic-aware abstraction. Further insights and video comparisons can be found in the supplementary video.

Recognizing the absence of appropriate metrics for numerically evaluating sketching, we conduct user studies to assess the performance of the generated video. In detail, for each of the 12 clips, we provide generated videos created by different methods for comparison. We then invite 25 individuals to rank the resulting videos in terms of semantic alignment (abstraction), temporal consistency (temporal), and overall quality (Overall), respectively. The order of the generated videos is shuffled, and participants score the results from 1 to 4 based on their ranking. As presented in Table 1, our method receives more favorable feedback from users when compared to the baseline CLIPasso [41], demon-

	Temporal \uparrow	Abstraction \uparrow	Overall \uparrow
Canny	2.65	2.58	2.51
HED	2.67	2.30	2.60
CLIPasso	2.13	2.41	2.31
Ours	2.58	2.74	2.71

Table 1. The mean opinion of the user studies.

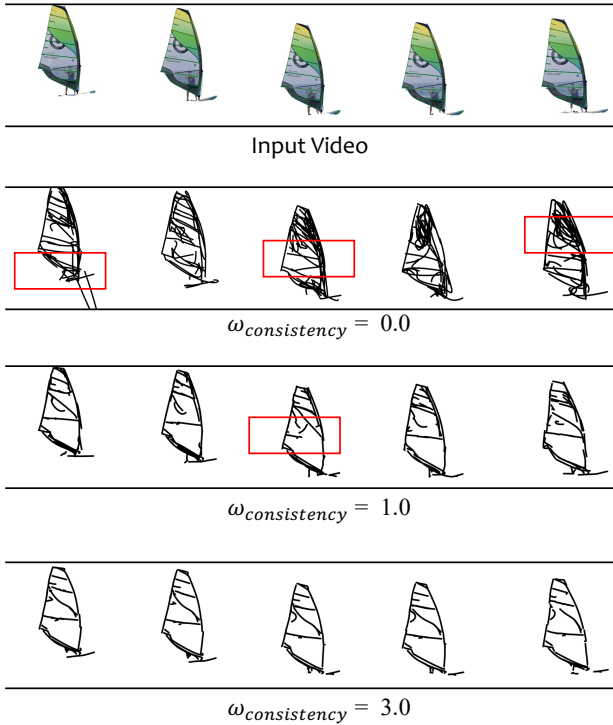


Figure 8. The importance of the proposed consistency loss.

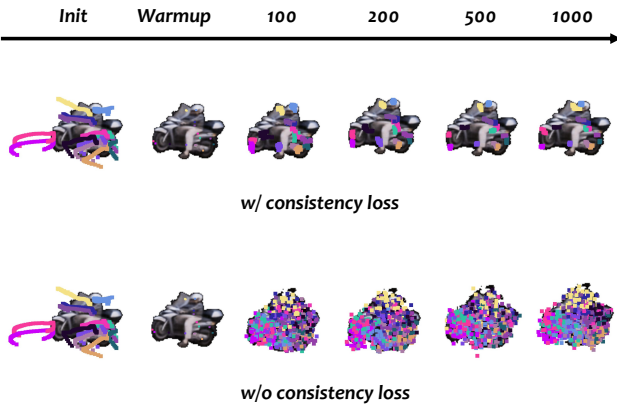


Figure 9. **Point Visualization.** To further support the effectiveness of the proposed consistency loss on the atlas, we visualize the location of the same curves (same color) on different frames during optimization. Kindly take note that the warmup points have been gathered, and it is recommended to view them with zoom in.

strating improvements across temporal consistency, semantic abstraction, and overall quality. Moreover, it’s noteworthy that our approach achieves enhanced semantic results with scores on par with those of edge detection methods in terms of temporal consistency.

4.2. Ablation Studies

Optimization Visualization. We introduce a novel consistency loss based on the trained atlas network. Here, we visualize the points on the global UV map (atlas) to gain a

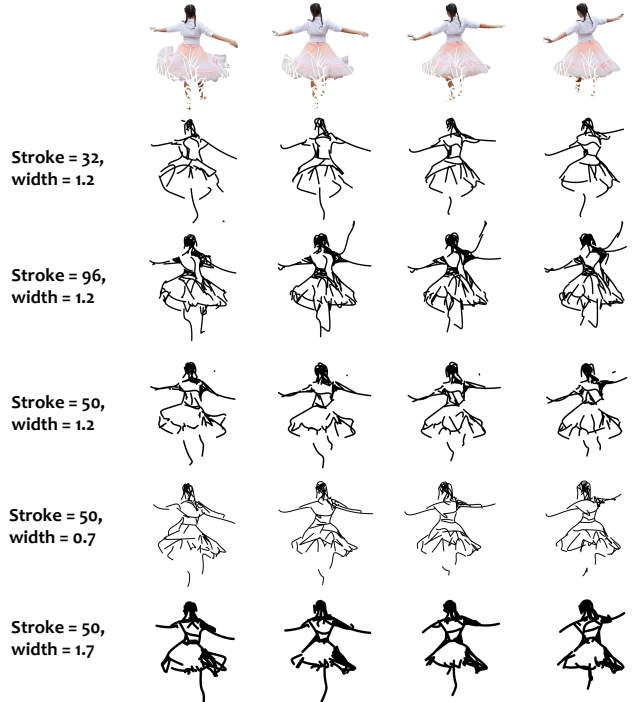


Figure 10. The ablations on the width and stroke numbers.

clearer understanding. As illustrated in Fig 9, points with the same index across multiple frames are represented in the same color. During the optimization process, the control points from different frames are appropriately positioned at the same points after the warming-up phase. Subsequently, we optimize these points using both the consistency loss and the semantic loss to ensure performance in terms of semantic alignment and coherence.

Consistency Weights. The novel consistency loss maintains temporal domain consistency through the trained atlas representation. In our ablation study, we investigate this loss using different values. As depicted in Fig. 8, when the consistency loss is excluded (*i.e.*, $\omega_{consistency} = 0$), the generated sketch exhibits distinct representations across frames. As we increment this parameter, the optimized results demonstrate enhanced stability.

Strokes Number and Width. We also show the SVG using different numbers and widths of the default strokes. Increasing the number of paths, as illustrated in Fig. 10, leads to the generation of sketches that capture more intricate details. For instance, the details of the dress and its movements become more prominent and well-defined, which reduces the level of abstraction. Likewise, adjusting the stroke width yields similar effects. Decreasing the stroke width during optimization emphasizes finer details within the strokes rather than the overall structure, resulting in a less abstract representation.



Figure 11. **Limitations.** When the motion is large and the object is complex, the generated atlas may not be accurate, causing temporal inconsistency.

4.3. Limitation

While our method excels at generating coherent and semantically rich videos, the limitations of the trained layer atlas [22] constrain the quality of the sketches. For instance, it faces challenges when representing the motion of non-rigid bodies. Additionally, during cases of self-occlusion, the generated abstract sketches may contain errors, often appearing as improper turns (as observed in the supplementary video). Furthermore, the generated sketches may exhibit some texture artifacts when the video undergoes significant motion or involves complex foreground elements. As depicted in Fig. 11, our proposed method exhibits artifacts when the male face shakes violently, and the atlas struggles to accurately represent the woman in the image. While some of these issues can be mitigated by subdividing the video into smaller sections and employing more layers, the accuracy of segmentation and the computational cost associated with multi-layer approaches remain challenges.

4.4. Conclusion

We present an optimization-based approach for generating sketch videos that maintain both semantic and temporal consistency. Our method facilitates the creation of sketching videos with the appropriate level of abstraction. Essentially, it includes a novel initialization technique for acquiring well-initialized points and a distinctive consistency loss derived from self-supervised video decomposition. These innovations empower us to craft sketch videos using simple Bézier curves. Since the resulting videos are composed using Scalable Vector Graphics, our proposed methods offer versatile applications in video editing and doodling, accommodating various sizes while preserving intricate details.

References

[1] P Arbeláez, M Maire, C Fowlkes, and J Malik. Contour detection and hierarchical image segmentation. *IEEE Transactions on Pattern Analysis and Machine Intelligence*, page 898–916, Aug 2010. 3

[2] Omer Bar-Tal, Dolev Ofri-Amar, Rafail Fridman, Yoni Kasten, and Tali Dekel. Text2live: Text-driven layered image and video editing. In *European Conference on Computer Vision*, pages 707–723. Springer, 2022. 4

[3] N. Ben-Zvi, J. Bento, Moshe Mahler, Jessica K. Hodgins, and Ariel Shamir. Line-drawing video stylization. *Computer Graphics Forum*, 35, 2016. 3

[4] Itamar Berger, Ariel Shamir, Moshe Mahler, Elizabeth Carter, and Jessica Hodgins. Style and abstraction in portrait sketching. *ACM Trans. Graph.*, 32(4), jul 2013. 2

[5] Nicolas Bonneel, James Tompkin, Kalyan Sunkavalli, Deqing Sun, Sylvain Paris, and Hanspeter Pfister. Blind video temporal consistency. *ACM Transactions on Graphics (Proceedings of SIGGRAPH Asia 2015)*, 34(6), 2015. 4

[6] John Canny. A computational approach to edge detection. *IEEE Transactions on Pattern Analysis and Machine Intelligence*, PAMI-8(6):679–698, 1986. 2, 3, 7

[7] Alexandre Carlier, Martin Danelljan, Alexandre Alahi, and Radu Timofte. Deepsvg: A hierarchical generative network for vector graphics animation. *Advances in Neural Information Processing Systems*, 33:16351–16361, 2020. 3

[8] Ayan Das, Yongxin Yang, Timothy Hospedales, Tao Xiang, and Yi-Zhe Song. Béziersketch: A generative model for scalable vector sketches. In *Computer Vision—ECCV 2020: 16th European Conference, Glasgow, UK, August 23–28, 2020, Proceedings, Part XXVI 16*, pages 632–647. Springer, 2020. 3

[9] Alexey Dosovitskiy, Lucas Beyer, Alexander Kolesnikov, Dirk Weissenborn, Xiaohua Zhai, Thomas Unterthiner, Mostafa Dehghani, Matthias Minderer, Georg Heigold, Sylvain Gelly, et al. An image is worth 16x16 words: Transformers for image recognition at scale. *arXiv preprint arXiv:2010.11929*, 2020. 6

[10] Patrick Esser, Johnathan Chiu, Parmida Atighehchian, Jonathan Granskog, and Anastasis Germanidis. Structure and content-guided video synthesis with diffusion models. *arXiv preprint arXiv:2302.03011*, 2023. 4

[11] Jakub Fišer, Ondřej Jamriška, Michal Lukáč, Eli Shechtman, Paul Asente, Jingwan Lu, and Daniel Šykora. Stylit: illumination-guided example-based stylization of 3d renderings. *ACM Transactions on Graphics (TOG)*, 35(4):1–11, 2016. 4

[12] Jakub Fišer, Ondřej Jamriška, David Simons, Eli Shechtman, Jingwan Lu, Paul Asente, Michal Lukáč, and Daniel Šykora. Example-based synthesis of stylized facial animations. *ACM Transactions on Graphics (TOG)*, 36(4):1–11, 2017. 4

- [13] Kevin Frans, Lisa Soros, and Olaf Witkowski. Clipdraw: Exploring text-to-drawing synthesis through language-image encoders. *Advances in Neural Information Processing Systems*, 35:5207–5218, 2022. 3
- [14] Leon A Gatys, Alexander S Ecker, and Matthias Bethge. Image style transfer using convolutional neural networks. In *Proceedings of the IEEE conference on computer vision and pattern recognition*, pages 2414–2423, 2016. 4
- [15] Yulia Gryaditskaya, Mark Sypsteyn, Jan Willem Hoftijzer, Sylvia Pont, Frédo Durand, and Adrien Bousseau. Opensketch: a richly-annotated dataset of product design sketches. *ACM Transactions on Graphics*, page 1–16, Nov 2019. 2
- [16] David Ha and Douglas Eck. A neural representation of sketch drawings, Apr 2017. 3
- [17] Kaiming He, Xiangyu Zhang, Shaoqing Ren, and Jian Sun. Deep residual learning for image recognition. In *Proceedings of the IEEE conference on computer vision and pattern recognition*, pages 770–778, 2016. 6
- [18] Shir Iluz, Yael Vinker, Amir Hertz, Daniel Berio, Daniel Cohen-Or, and Ariel Shamir. Word-as-image for semantic typography. *arXiv preprint arXiv:2303.01818*, 2023. 3
- [19] Ondřej Jamriška, Šárka Sochorová, Ondřej Texler, Michal Lukáč, Jakub Fišer, Jingwan Lu, Eli Shechtman, and Daniel Šýkora. Stylizing video by example. *ACM Trans. Graph.*, 38(4), jul 2019. 4
- [20] Justin Johnson, Alexandre Alahi, and Li Fei-Fei. Perceptual losses for real-time style transfer and super-resolution. In *Computer Vision—ECCV 2016: 14th European Conference, Amsterdam, The Netherlands, October 11–14, 2016, Proceedings, Part II 14*, pages 694–711. Springer, 2016. 4
- [21] Moritz Kampelmueller and Axel Pinz. Synthesizing human-like sketches from natural images using a conditional convolutional decoder. In *Proceedings of the IEEE/CVF winter conference on applications of computer vision*, pages 3203–3211, 2020. 2
- [22] Yoni Kasten, Dolev Ofri, Oliver Wang, and Tali Dekel. Layered neural atlases for consistent video editing. *ACM Transactions on Graphics (TOG)*, 40(6):1–12, 2021. 2, 4, 9
- [23] Levon Khachatryan, Andranik Movsisyan, Vahram Tadevosyan, Roberto Henschel, Zhangyang Wang, Shant Navasardyan, and Humphrey Shi. Text2video-zero: Text-to-image diffusion models are zero-shot video generators. *arXiv preprint arXiv:2303.13439*, 2023. 4
- [24] Wei-Sheng Lai, Jia-Bin Huang, Oliver Wang, Eli Shechtman, Ersin Yumer, and Ming-Hsuan Yang. Learning blind video temporal consistency. In *Proceedings of the European conference on computer vision (ECCV)*, pages 170–185, 2018. 4
- [25] Chenyang Lei, Xuanchi Ren, Zhaoxiang Zhang, and Qifeng Chen. Blind video deflickering by neural filtering with a flawed atlas. In *Proceedings of the IEEE/CVF Conference on Computer Vision and Pattern Recognition (CVPR)*, June 2023. 2, 4
- [26] Chenyang Lei, Yazhou Xing, and Qifeng Chen. Blind video temporal consistency via deep video prior. *Advances in Neural Information Processing Systems*, 33:1083–1093, 2020. 2, 4
- [27] Chenyang Lei, Yazhou Xing, Hao Ouyang, and Qifeng Chen. Deep video prior for video consistency and propagation. *IEEE Transactions on Pattern Analysis and Machine Intelligence*, 45(1):356–371, 2022. 4
- [28] Mengtian Li, Zhe Lin, Radomir Mech, Ersin Yumer, and Deva Ramanan. Photo-sketching: Inferring contour drawings from images. In *2019 IEEE Winter Conference on Applications of Computer Vision (WACV)*, pages 1403–1412. IEEE, 2019. 2
- [29] Tzu-Mao Li, Michal Lukáč, Gharbi Michaël, and Jonathan Ragan-Kelley. Differentiable vector graphics rasterization for editing and learning. *ACM Trans. Graph. (Proc. SIGGRAPH Asia)*, 39(6):193:1–193:15, 2020. 2, 3, 5
- [30] Shanchuan Lin, Linjie Yang, Imran Saleemi, and Soumyadip Sengupta. Robust high-resolution video matting with temporal guidance. *CoRR*, 2021. 7
- [31] Shaoteng Liu, Yuechen Zhang, Wenbo Li, Zhe Lin, and Jiaya Jia. Video-p2p: Video editing with cross-attention control. *arXiv:2303.04761*, 2023. 4
- [32] Jordi Pont-Tuset, Federico Perazzi, Sergi Caelles, Pablo Arbeláez, Alex Sorkine-Hornung, and Luc Van Gool. The 2017 davis challenge on video object segmentation. *arXiv preprint arXiv:1704.00675*, 2017. 7
- [33] Chenyang Qi, Xiaodong Cun, Yong Zhang, Chenyang Lei, Xintao Wang, Ying Shan, and Qifeng Chen. Fatezero: Fusing attentions for zero-shot text-based video editing. *arXiv:2303.09535*, 2023. 4
- [34] Alec Radford, Jong Wook Kim, Chris Hallacy, Aditya Ramesh, Gabriel Goh, Sandhini Agarwal, Girish Sastry, Amanda Askell, Pamela Mishkin, Jack Clark, et al. Learning transferable visual models from natural language supervision. In *International conference on machine learning*, pages 8748–8763. PMLR, 2021. 2, 3, 5, 6

- [35] Pradyumna Reddy, Michael Gharbi, Michal Lukac, and Niloy J Mitra. Im2vec: Synthesizing vector graphics without vector supervision. In *Proceedings of the IEEE/CVF Conference on Computer Vision and Pattern Recognition*, pages 7342–7351, 2021. 3
- [36] Robin Rombach, Andreas Blattmann, Dominik Lorenz, Patrick Esser, and Björn Ommer. High-resolution image synthesis with latent diffusion models, 2021. 3, 4
- [37] Roman Suvorov, Elizaveta Logacheva, Anton Mashikhin, Anastasia Remizova, Arsenii Ashukha, Aleksei Silvestrov, Naejin Kong, Harshith Goka, Kiwoong Park, and Victor Lempitsky. Resolution-robust large mask inpainting with fourier convolutions. *arXiv preprint arXiv:2109.07161*, 2021. 6
- [38] Zachary Teed and Jia Deng. Raft: Recurrent all-pairs field transforms for optical flow. In *Computer Vision—ECCV 2020: 16th European Conference, Glasgow, UK, August 23–28, 2020, Proceedings, Part II 16*, pages 402–419. Springer, 2020. 6
- [39] Yingtao Tian and David Ha. *Modern Evolution Strategies for Creativity: Fitting Concrete Images and Abstract Concepts*, page 275–291. Springer, Apr 2022. 3
- [40] Yael Vinker, Yuval Alaluf, Daniel Cohen-Or, and Ariel Shamir. Clipascene: Scene sketching with different types and levels of abstraction. In *Proceedings of the IEEE/CVF International Conference on Computer Vision (ICCV)*, pages 4146–4156, October 2023. 2, 3
- [41] Yael Vinker, Ehsan Pajouheshgar, JessicaY. Bo, RomanChristian Bachmann, AmitHaim Bermano, Daniel Cohen-Or, Amir Zamir, and Ariel Shamir. Clipasso: Semantically-aware object sketching. *ACM Trans. Graph.*, 2022. 2, 3, 5, 6, 7
- [42] Ting-Chun Wang, Ming-Yu Liu, Jun-Yan Zhu, Guilin Liu, Andrew Tao, Jan Kautz, and Bryan Catanzaro. Video-to-video synthesis. In *Advances in Neural Information Processing Systems (NeurIPS)*, 2018. 4, 6
- [43] Holger Winnemöller, Jan Eric Kyprianidis, and Sven C Olsen. Xdog: An extended difference-of-gaussians compendium including advanced image stylization. *Computers & Graphics*, 36(6):740–753, 2012. 2, 5
- [44] Jay Zhangjie Wu, Yixiao Ge, Xintao Wang, Stan Weixian Lei, Yuchao Gu, Wynne Hsu, Ying Shan, Xiaohu Qie, and Mike Zheng Shou. Tune-a-video: One-shot tuning of image diffusion models for text-to-video generation. *arXiv preprint arXiv:2212.11565*, 2022. 4
- [45] Ronghuan Wu, Wanchao Su, Kede Ma, and Jing Liao. Iconshop: Text-based vector icon synthesis with autoregressive transformers. *arXiv preprint arXiv:2304.14400*, 2023. 3
- [46] Saining Xie and Zhuowen Tu. Holistically-nested edge detection. In *Proceedings of the IEEE international conference on computer vision*, pages 1395–1403, 2015. 2, 3, 7
- [47] Peng Xu, TimothyM. Hospedales, Qiyue Yin, Yi-Zhe Song, Tao Xiang, and Liang Wang. Deep learning for free-hand sketch: A survey and a toolbox. *arXiv: Computer Vision and Pattern Recognition*, Jan 2020. 2
- [48] Shuai Yang, Liming Jiang, Ziwei Liu, and Chen Change Loy. Vtoonify: Controllable high-resolution portrait video style transfer. *ACM Transactions on Graphics (TOG)*, 41(6):1–15, 2022. 4
- [49] Emilie Yu, Kevin Blackburn-Matzen, Cuong Nguyen, Oliver Wang, Rubaiat Habib Kazi, and Adrien Bousseau. Videodoodles: Hand-drawn animations on videos with scene-aware canvases. *ACM Transactions on Graphics (TOG)*, 42:1 – 12, 2023. 3
- [50] Richard Zhang, Phillip Isola, Alexei A Efros, Eli Shechtman, and Oliver Wang. The unreasonable effectiveness of deep features as a perceptual metric. In *CVPR*, 2018. 4